Impact of the electronic band structure in high-harmonic generation spectra of solids: supplementary material

Nicolas Tancogne-Dejean,[1,2,*] Oliver D. Mücke,[3,4] Franz X. Kärtner,[3,5,4,6] and Angel Rubio[1,2,3,5,†]

[1] *Max Planck Institute for the Structure and Dynamics of Matter, Luruper Chaussee 149, 22761 Hamburg, Germany*
[2] *European Theoretical Spectroscopy Facility (ETSF)*
[3] *Center for Free-Electron Laser Science CFEL, Deutsches Elektronen-Synchrotron DESY, Notkestraße 85, 22607 Hamburg, Germany*
[4] *The Hamburg Center for Ultrafast Imaging, Luruper Chaussee 149, 22761 Hamburg, Germany*
[5] *Physics Department, University of Hamburg, Luruper Chaussee 149, 22761 Hamburg, Germany*
[6] *Research Laboratory of Electronics, Massachusetts Institute of Technology, 77 Massachusetts Avenue, Cambridge, MA 02139, USA*

COMPARISON OF THE JOINT DOS AND THE HHG SPECTRA FOR BULK ALAS

In order to show that our conclusions are valid not only for cubic silicon, we also performed calculations for bulk AlAs, which has a zinc-blende crystal structure. We used a real-space spacing of 0.344 atomic units and an optimized 32×32×32 grid shifted four times to sample the BZ. The peak intensity inside matter is taken to be $I_0 = 10^{11}\,\mathrm{W\,cm^{-2}}$, and the carrier wavelength λ is 3000 nm, corresponding to a carrier photon energy of 0.43 eV. The comparison between the joint DOS and the HHG spectra of AlAs is presented in Fig. 1.

As expected, we obtain that when the JDOS is low, the HHG exhibits clean harmonics, whereas higher JDOS is associated with noisy harmonics. Similarly to the case of bulk silicon, we see that the noisy region (orange shaded area) is suppressed, thus recovering clean odd and even harmonics (green shaded area), when the JDOS is very low.

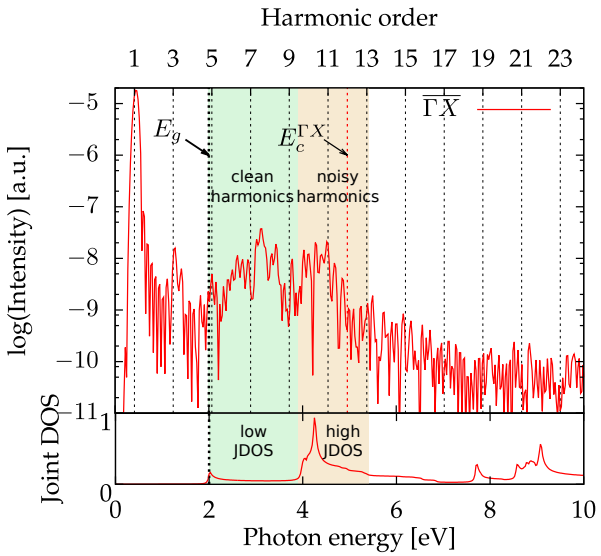

FIG. 1. HHG spectra for the $\overline{\Gamma X}$ polarization direction (red line). The bottom panel shows the corresponding joint DOS. The red and blue dashed lines indicate the position of the cutoff energy (E_c) for $\overline{\Gamma X}$. The shaded areas are guides to the eye.

HHG SPECTRA AT HIGHER INTENSITY

We performed calculations at higher intensity $I_0 = 10^{12}\,\mathrm{W\,cm^{-2}}$. In order to get converged results, we employed a denser 38×38×38 grid shifted four times to sample the BZ.

As electrons explore a larger part of the Brillouin zone, the joint DOS is higher and no clean odd-harmonic structure is observed above the band gap, see Fig. 2.

We also note that the increase of the cutoff photon energy is consistent with a linear scaling in the electric field strength, as observed experimentally [1].

EFFECT OF THE MATERIAL BAND GAP

In order to study the effect of the material band gap, we added in our time-dependent Kohn-Sham Hamiltonian a scissor operator, allowing us to artificially open the band gap by any value by shifting the conduction bands to higher energy. We have then simulated an artificial bulk silicon, increasing the band gap by 3.0 eV. We observe in Fig. 3 a region of clean odd-harmonics below the band gap, which is increased while increasing the band gap. This confirms once again that the interband contribution is suppressed for photon energies below the band gap. We also observe that the cutoff photon energy increases by the value of the bap opening ($\Delta = 3.0$ eV).

COMPARISON BETWEEN $\overline{\Gamma X}$, $\overline{\Gamma K}$ AND $\overline{\Gamma L}$

On Fig. 4, we compare the HHG spectra obtained for $I_0 = 10^{11}\,\mathrm{W\,cm^{-2}}$, and the carrier wavelength λ is 3000 nm, for polarization along the $\overline{\Gamma X}$, $\overline{\Gamma K}$, and $\overline{\Gamma L}$ di-

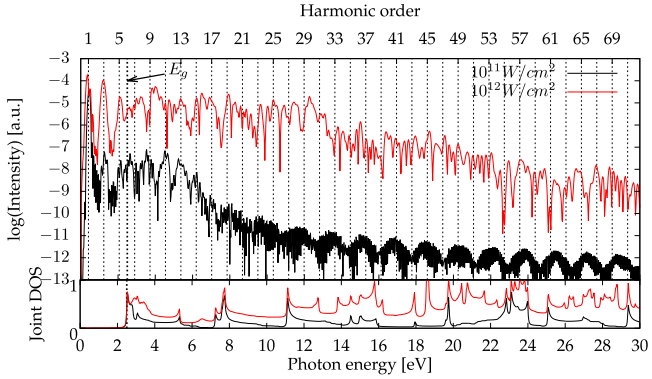

FIG. 2. Top panel: HHG spectra from bulk silicon computed within the local-density approximation, with laser polarization along the $\overline{\Gamma X}$ direction for $I_0 = 10^{11}\mathrm{W\,cm^{-2}}$ (black line) and $I_0 = 10^{12}\mathrm{W\,cm^{-2}}$ (red line). Bottom panel: Comparison of the joint DOS computed for the region explored by the electron for $I_0 = 10^{11}\mathrm{W\,cm^{-2}}$ (black line) and $I_0 = 10^{12}\mathrm{W\,cm^{-2}}$ (red line).

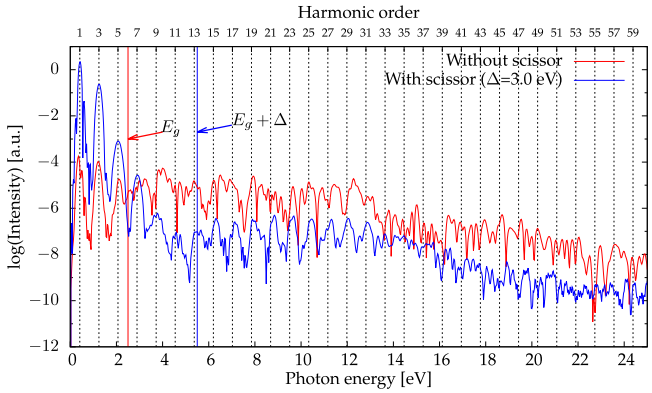

FIG. 3. HHG spectra from bulk silicon computed within the local-density approximation, with laser polarization along the $\overline{\Gamma X}$ direction for $I_0 = 10^{12}\mathrm{W\,cm^{-2}}$, without scissor operator (red line) and including a scissor correction (Δ) of 3.0 eV (blue line).

rections.

DERIVATION OF THE ANALYTICAL MODEL

We consider a general interacting many-electron Hamiltonian $\hat{H}$ of the form

$$\hat{H}(t) = \hat{T} + \hat{V}(t) + \hat{W}, \tag{1}$$

where $\hat{T}$ is the kinetic energy, $\hat{V}(t)$ is the time-dependent external laser potential, and $\hat{W}$ is the electron-electron Coulomb interaction (the ionic motion is not considered here for the sake of simplicity).
In second quantization, we have [2, 3]

$$\hat{T} = -\frac{1}{2}\int d^3\mathbf{r}\hat{\psi}^\dagger(\mathbf{r})\nabla^2\hat{\psi}(\mathbf{r}), \tag{2}$$

$$\hat{V}(t) = \int d^3\mathbf{r}\hat{\psi}^\dagger(\mathbf{r})v(\mathbf{r},t)\hat{\psi}(\mathbf{r}), \tag{3}$$

$$\hat{W} = \int d^3\mathbf{r}\int d^3\mathbf{r}' w(|\mathbf{r}-\mathbf{r}'|)\hat{\psi}^\dagger(\mathbf{r})\hat{\psi}^\dagger(\mathbf{r}')\hat{\psi}(\mathbf{r}')\hat{\psi}(\mathbf{r}) \tag{4}$$

The current operator is defined by

$$\hat{\mathbf{j}}(\mathbf{r}) = \frac{1}{2i}\{\hat{\psi}^\dagger(\mathbf{r})\nabla\hat{\psi}(\mathbf{r}) - (\nabla\hat{\psi}^\dagger(\mathbf{r}))\hat{\psi}(\mathbf{r})\}. \tag{5}$$

Its equation of motion is given by [2]

$$\frac{\partial}{\partial t}\mathbf{j}(\mathbf{r},t) = -i\langle\Psi(t)|[\hat{\mathbf{j}}(\mathbf{r}), \hat{H}(t)]|\Psi(t)\rangle, \tag{6}$$

where $|\Psi(t)\rangle$ is the state evolving from the initial state $|\Psi_0\rangle$ under the influence of $\hat{H}(t)$. Following Refs. [2, 3], the equation of motion for the total microscopic current can be rewritten as

$$\frac{\partial}{\partial t}\mathbf{j}(\mathbf{r},t) = -n(\mathbf{r},t)\nabla v(\mathbf{r},t) + \Pi^{\mathrm{kin}}(\mathbf{r},t) + \Pi^{\mathrm{int}}(\mathbf{r},t), \tag{7}$$

where $\Pi^{\mathrm{kin}}(\mathbf{r},t)$ and $\Pi^{\mathrm{int}}(\mathbf{r},t)$ are the kinetic and the interaction contributions to the momentum-stress tensor [2, 3]. In second quantization, the k-component of $\Pi^{\mathrm{kin}}(\mathbf{r},t)$ and $\Pi^{\mathrm{int}}(\mathbf{r},t)$ are given respectively by

$$\Pi^{\mathrm{kin}}_k(\mathbf{r},t) = \langle\Psi(t)|\frac{1}{2}\sum_i \partial_i\{\partial_i\hat{\psi}^\dagger(\mathbf{r})\partial_k\hat{\psi}(\mathbf{r}) + \partial_k\hat{\psi}^\dagger(\mathbf{r})\partial_i\hat{\psi}(\mathbf{r})$$

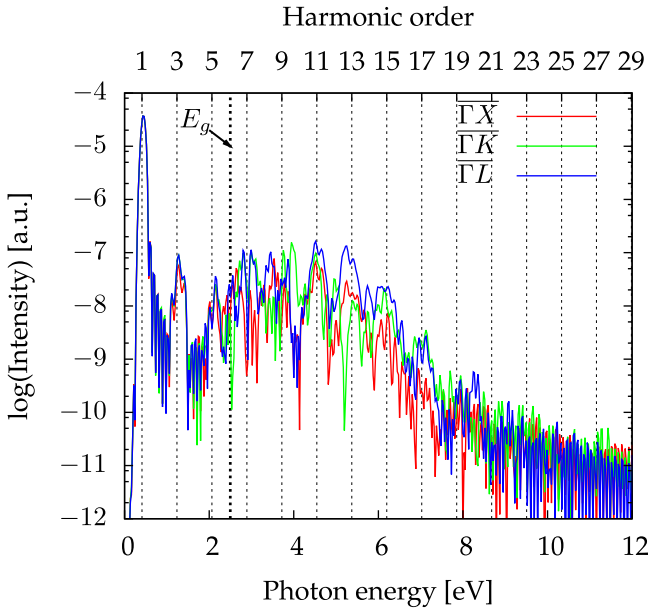

FIG. 4. HHG spectra from bulk silicon computed within the local-density approximation, for $I_0 = 10^{11}\mathrm{W\,cm^{-2}}$, and the carrier wavelength λ is 3000 nm, with laser polarization along the $\overline{\Gamma X}$ (red line), $\overline{\Gamma K}$ (green line), and $\overline{\Gamma L}$ (blue line) directions.

$$-\frac{1}{2}\partial_i\partial_k[\hat{\psi}^\dagger(\mathbf{r})\hat{\psi}(\mathbf{r})]\}|\Psi(t)\rangle$$

and

$$\Pi_k^{\mathrm{int}}(\mathbf{r},t) = \langle\Psi(t)|\int d^3\mathbf{r}'\hat{\psi}^\dagger(\mathbf{r})\hat{\psi}^\dagger(\mathbf{r}')\partial_k\, w(|\mathbf{r}-\mathbf{r}'|) \times\hat{\psi}(\mathbf{r}')\hat{\psi}(\mathbf{r})|\Psi(t)\rangle.$$

Also, $n(\mathbf{r},t)$ is the time-dependent electronic density of the system driven by the external strong laser pulse $\mathbf{E}(t)$, which is given by

$$n(\mathbf{r},t) = \langle\Psi(t)|\hat{n}(\mathbf{r})|\Psi(t)\rangle, \tag{8}$$

with $\hat{n}(\mathbf{r}) = \hat{\psi}^\dagger(\mathbf{r})\hat{\psi}(\mathbf{r})$.
This equation just represents the local momentum conservation law, and shows that only external forces contribute to the total momentum, in accordance to Newton's third law. As these two contributions to the momentum stress-tensor are internal forces [3], Eq. (7) reduces to

$$\frac{\partial}{\partial t}\int_\Omega d^3\mathbf{r}\,\mathbf{j}(\mathbf{r},t) = -\int_\Omega d^3\mathbf{r}\,n(\mathbf{r},t)\nabla v(\mathbf{r},t), \tag{9}$$

where Ω denotes the volume of the physical system. In here the external potential $v(\mathbf{r},t)$ accounts for both the electron-nuclei potential ($v_0(\mathbf{r})$) and the externally applied time-dependent laser field. In the velocity gauge, we have

$$v(\mathbf{r},t) = v_0(\mathbf{r}) + \phi(\mathbf{r},t) + \frac{1}{2c^2}\mathbf{A}^2(\mathbf{r},t) - \frac{1}{2c}\big(\nabla.\,\mathbf{A}(\mathbf{r},t) + \mathbf{A}(\mathbf{r},t).\,\nabla\big), \tag{10}$$

where ϕ and $\mathbf{A}$ are respectively the scalar and vector potentials, related to the electric field by

$$\mathbf{E}(\mathbf{r},t) = \frac{1}{c}\frac{\partial}{\partial t}\mathbf{A}(\mathbf{r},t) - \frac{\partial}{\partial\mathbf{r}}\phi(\mathbf{r},t). \tag{11}$$

The simplification of the equation of motion of the microscopic current to the Lorentz force is shown in detail in Ref. [3] and is therefore not reproduced here.
Using the current expression for the HHG spectra, namely $\mathrm{HHG}(\omega) = \left|\mathrm{FT}\left\{\int_\Omega d^3\mathbf{r}\,\frac{\partial}{\partial t}\mathbf{j}(\mathbf{r},t)\right\}\right|^2$, and plugging now Eq. (9), we obtain, a general expression for the HHG spectra

$$\mathrm{HHG}(\omega)\propto\left|\mathrm{FT}\left\{\int_\Omega d^3\mathbf{r}\left(n(\mathbf{r},t)\nabla v_0(\mathbf{r}) + n(\mathbf{r},t)\mathbf{E}(\mathbf{r},t) + \frac{\mathbf{j}(\mathbf{r},t)\times\mathbf{B}(\mathbf{r},t)}{c}\right)\right\}\right|^2, \tag{12}$$

where the last two terms correspond to the Lorentz force exerted by the external laser on the electronic system [3]. If we now make the dipole approximation, Eq. (12) further simplifies and we finally get

$$\mathrm{HHG}(\omega)\propto\left|\mathrm{FT}\left\{\int_\Omega d^3\mathbf{r}\,n(\mathbf{r},t)\nabla v_0(\mathbf{r})\right\} + N_e\mathbf{E}(\omega)\right|^2. \tag{13}$$

* nicolas.tancogne-dejean@mpsd.mpg.de
† angel.rubio@mpsd.mpg.de

[1] S. Ghimire, A. D. DiChiara, E. Sistrunk, P. Agostini, L. F. DiMauro, and D. A. Reis, Nature Physics **7**, 138 (2011).
[2] R. van Leeuwen, Phys. Rev. Lett. **82**, 3863 (1999).
[3] G. Stefanucci and R. van Leeuwen, *Nonequilibrium Many-Body Theory of Quantum Systems: A Modern Introduction* (Cambridge University Press, 2013).